Supporting information for

Conformationally Dynamic Titanium and Zirconium Cationic Complexes of Bis(naphthoxy)pyridine ligands: Structure, "Oscillation" and Olefin Polymerization Catalysis

Liana Annunziata, Thierry Roisnel, Abbas Razavi, Jean-François Carpentier,* and Evgueni Kirillov*

* Corresponding authors: Fax: (+33)(0)223-236-939. E-mail: jean-francois.carpentier@univ-rennes1.fr; evgueni.kirillov@univ-rennes1.fr.

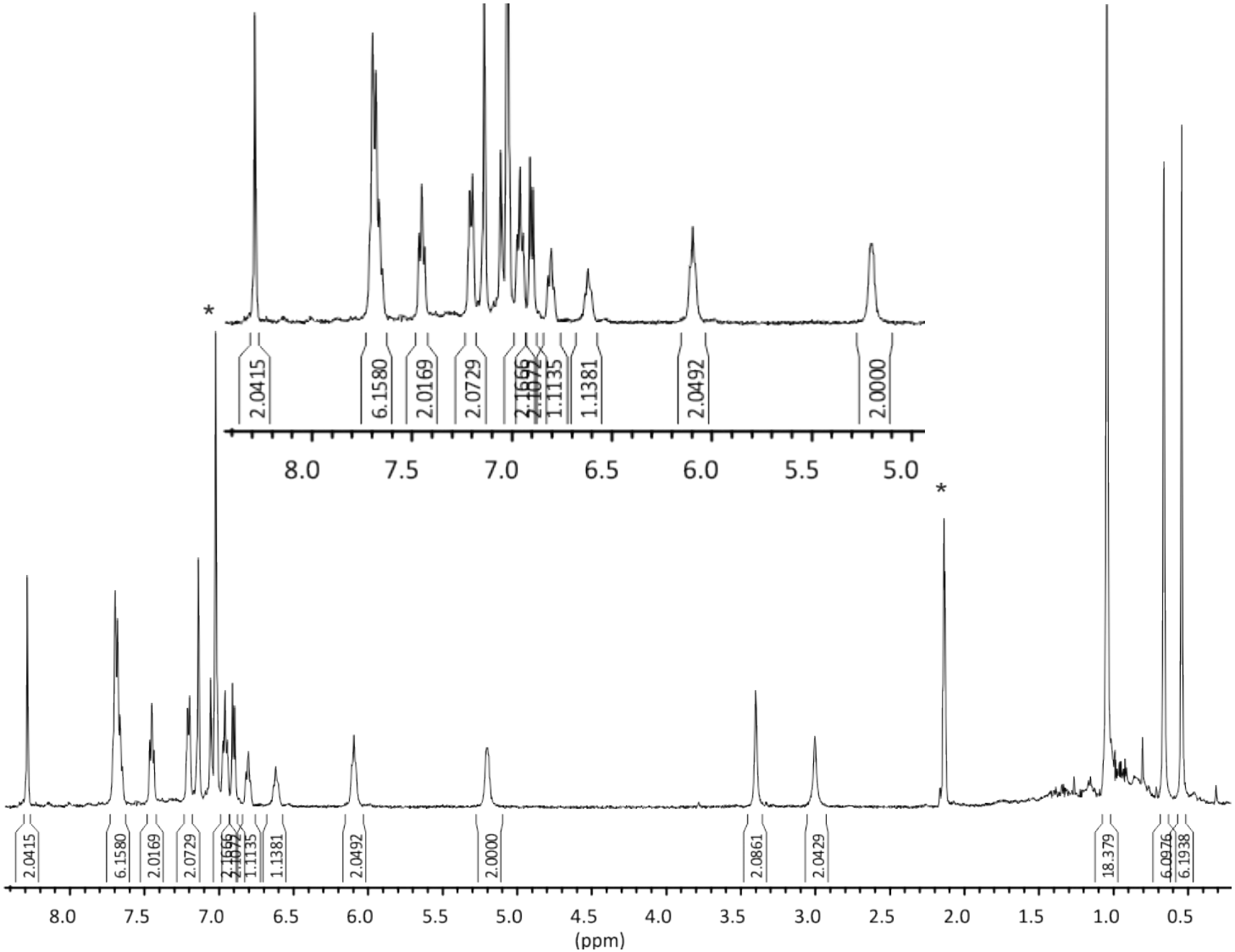

Figure S1. ^{1}H NMR spectrum (500 MHz, toluene-d_8, 25 °C) of complex {ONO^{SiMe2tBu}}Ti(CH_2Ph)(η^6-Ph)$CH_2B(C_6F_5)_3$ (**2-Ti**) (* stand for solvent peaks).

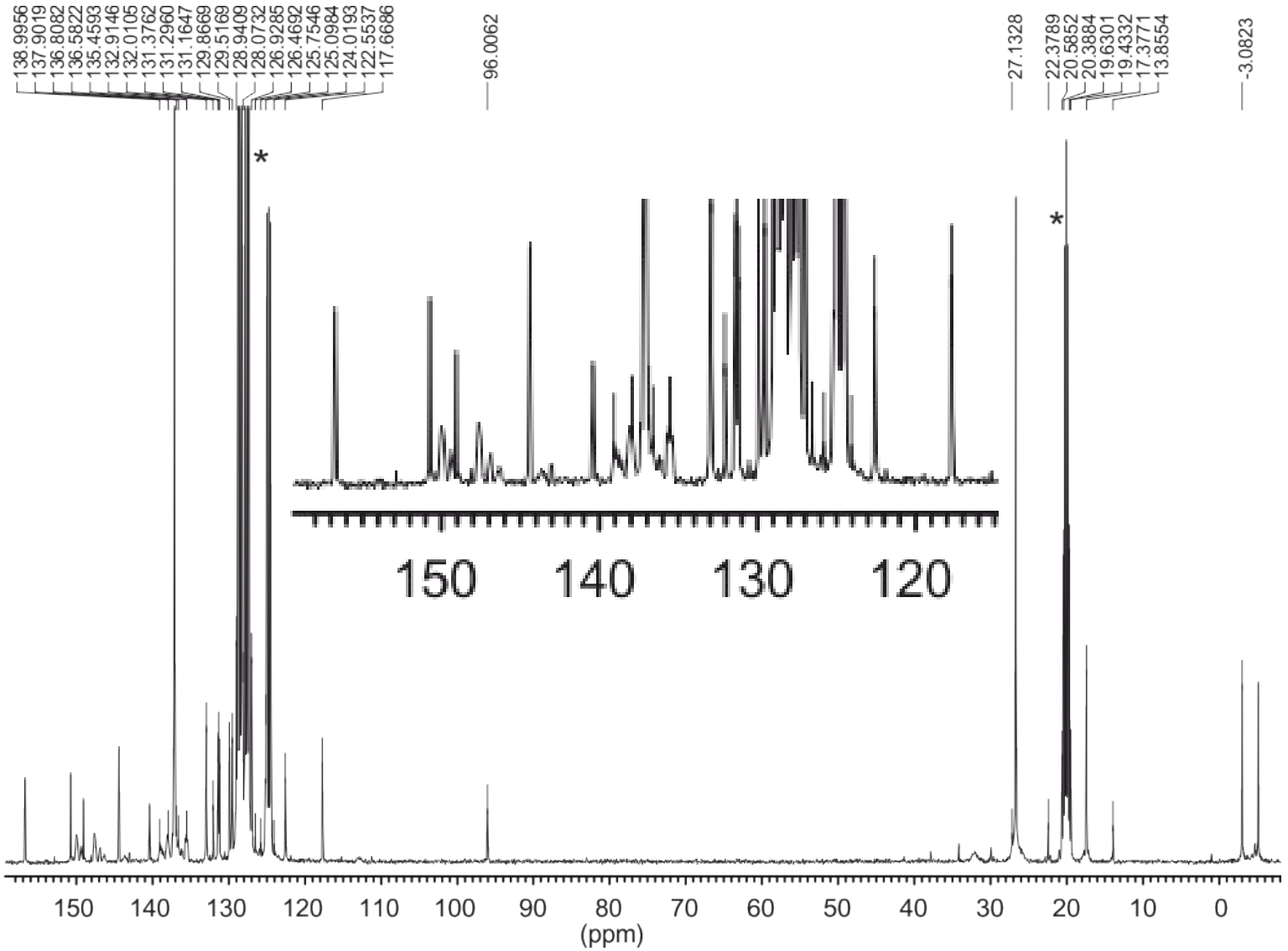

Figure S2. $^{13}C\{^{1}H\}$ NMR spectrum (100 MHz, toluene-d_8, 25 °C) of complex {ONO^{SiMe2tBu}}Ti(CH_2Ph)(η^6-Ph)$CH_2B(C_6F_5)_3$ (**2-Ti**) (* stand for solvent peaks).

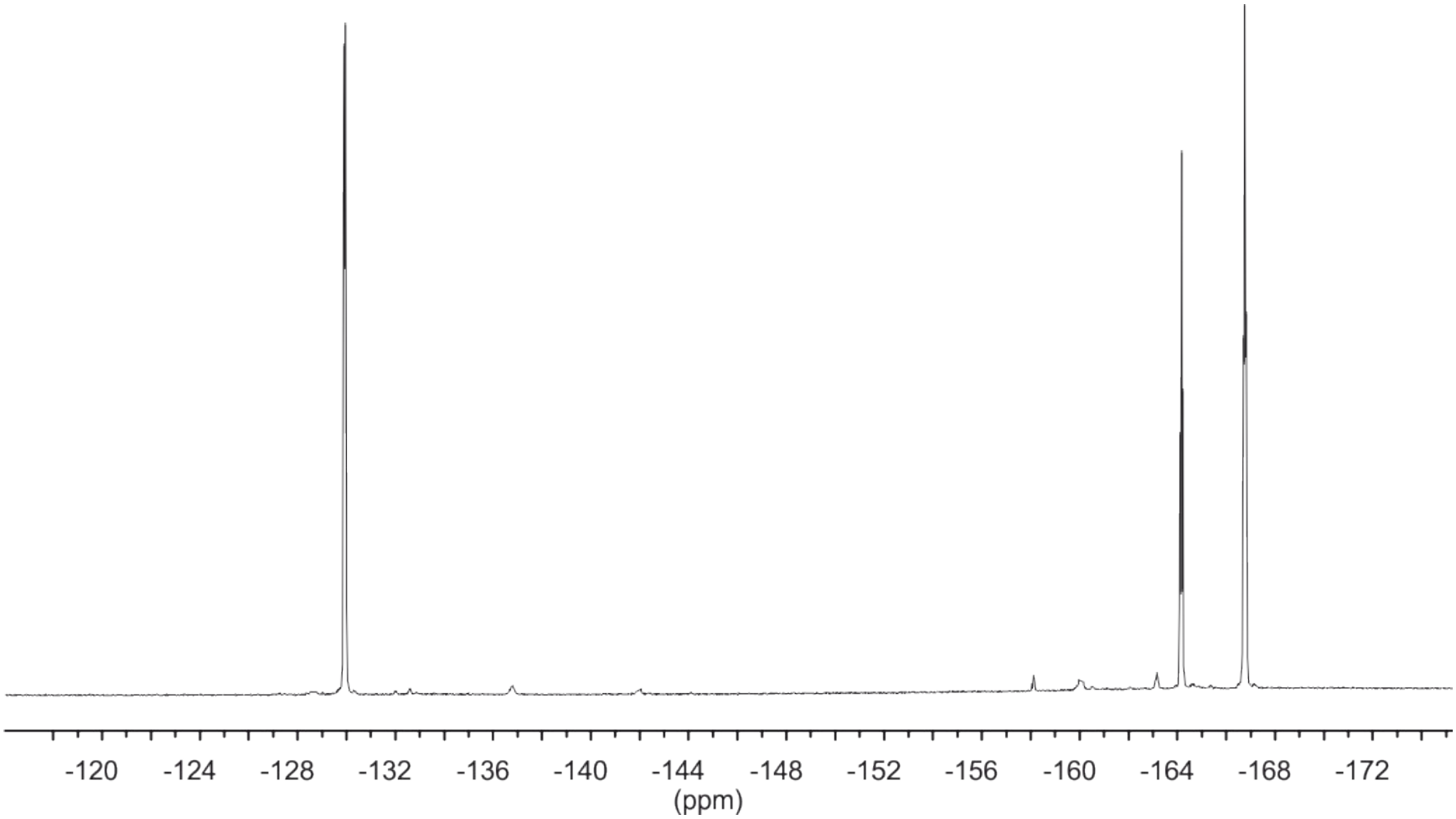

Figure S3. $^{19}F\{^{1}H\}$ NMR spectrum (376 MHz, toluene-d_8, 25 °C) of complex {ONO^{SiMe2tBu}}Ti(CH_2Ph)(η^6-Ph)$CH_2B(C_6F_5)_3$ (**2-Ti**).

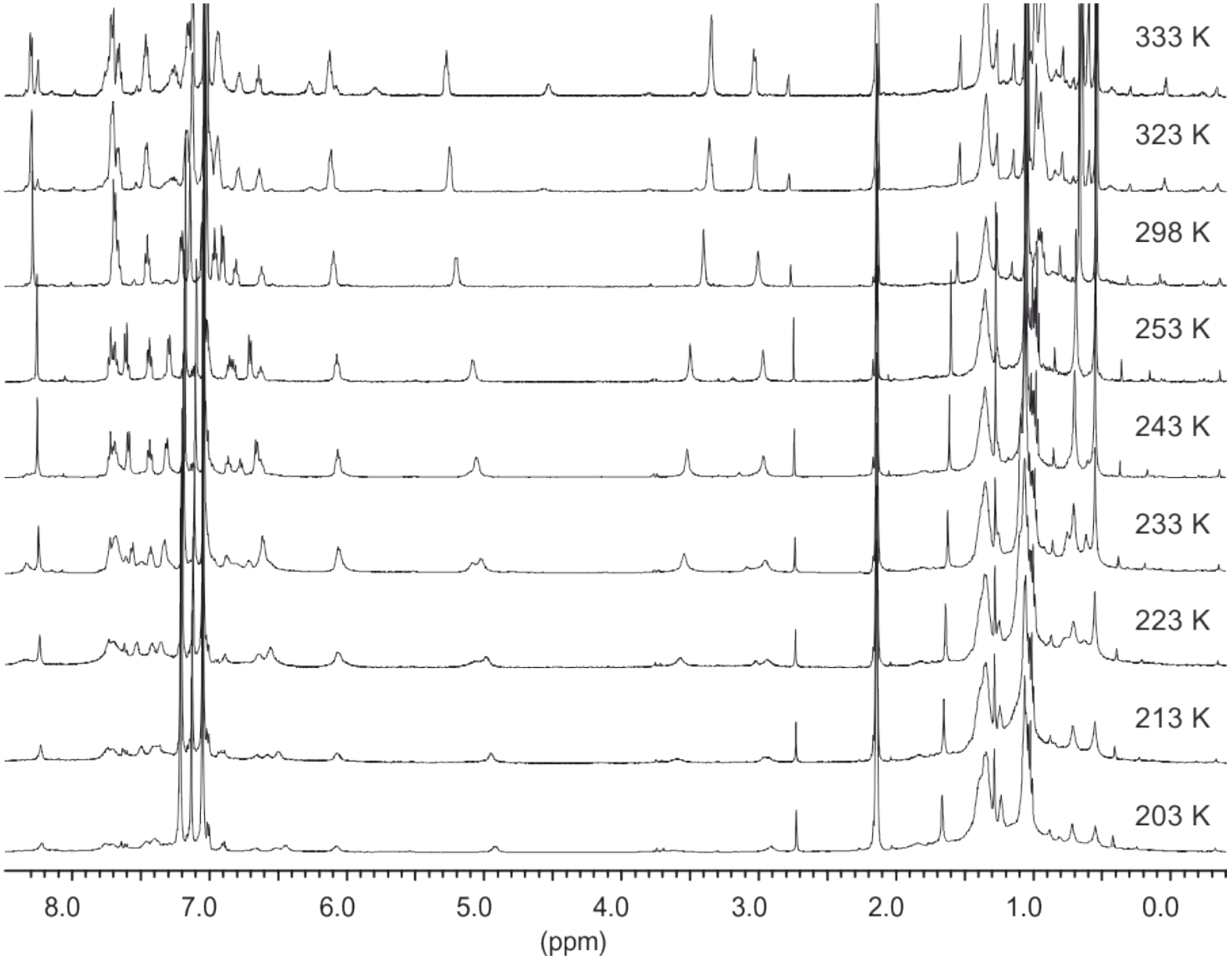

Figure S4. Stack plot of ^{1}H NMR spectra (500 MHz, toluene-d_8) of complex {ONO$^{\mathrm{SiMe2}t\mathrm{Bu}}$}Ti($CH_2$Ph)($\eta^6$-Ph)$CH_2B(C_6F_5)_3$ (**2-Ti**).

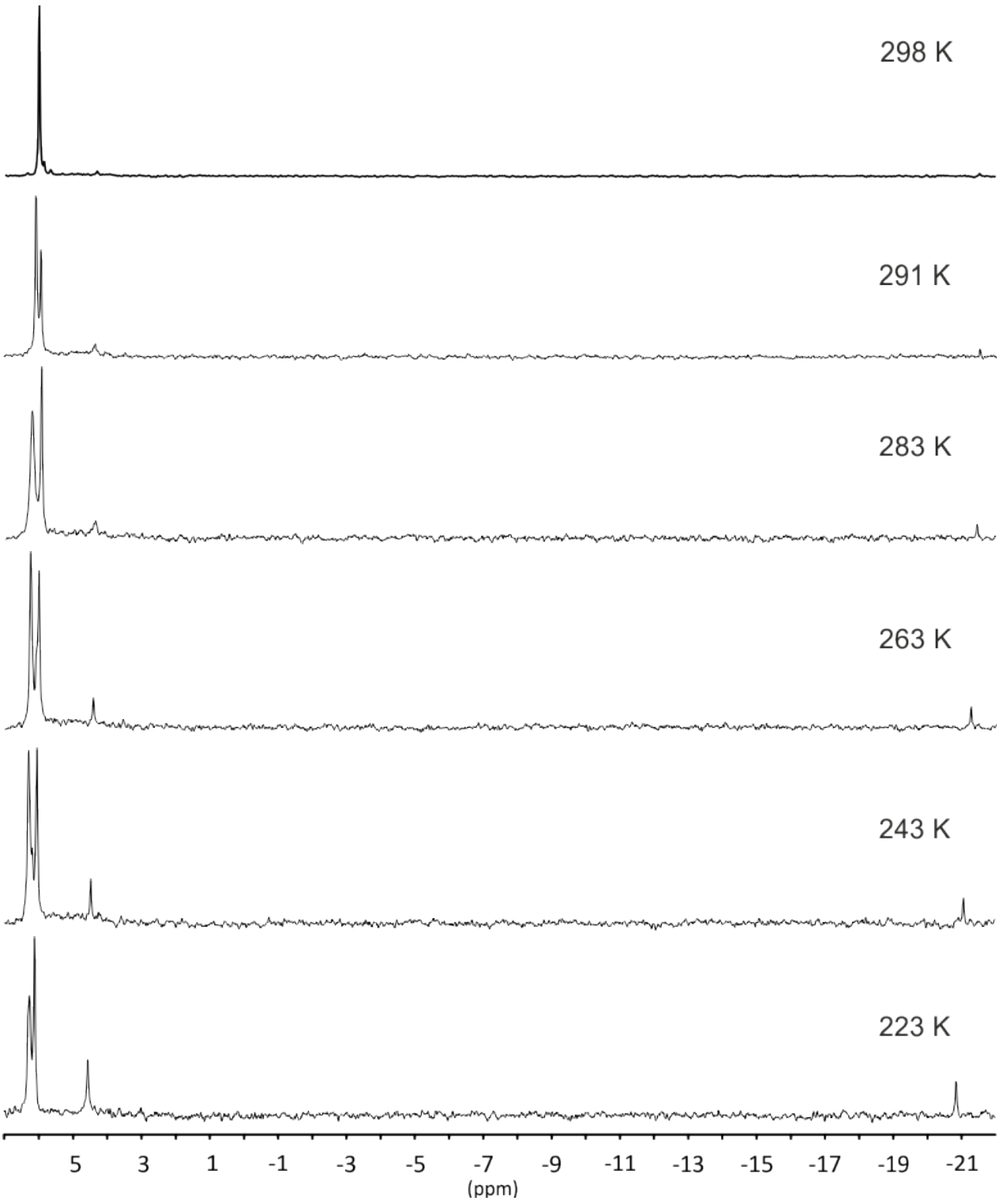

Figure S5. Stack plot of $^{29}Si\{^{1}H\}$ NMR spectra (79.5 MHz, toluene-d_8) of complex $\{ONO^{SiMe2tBu}\}Ti(CH_2Ph)(\eta^6\text{-}Ph)CH_2B(C_6F_5)_3$ (**2-Ti**).

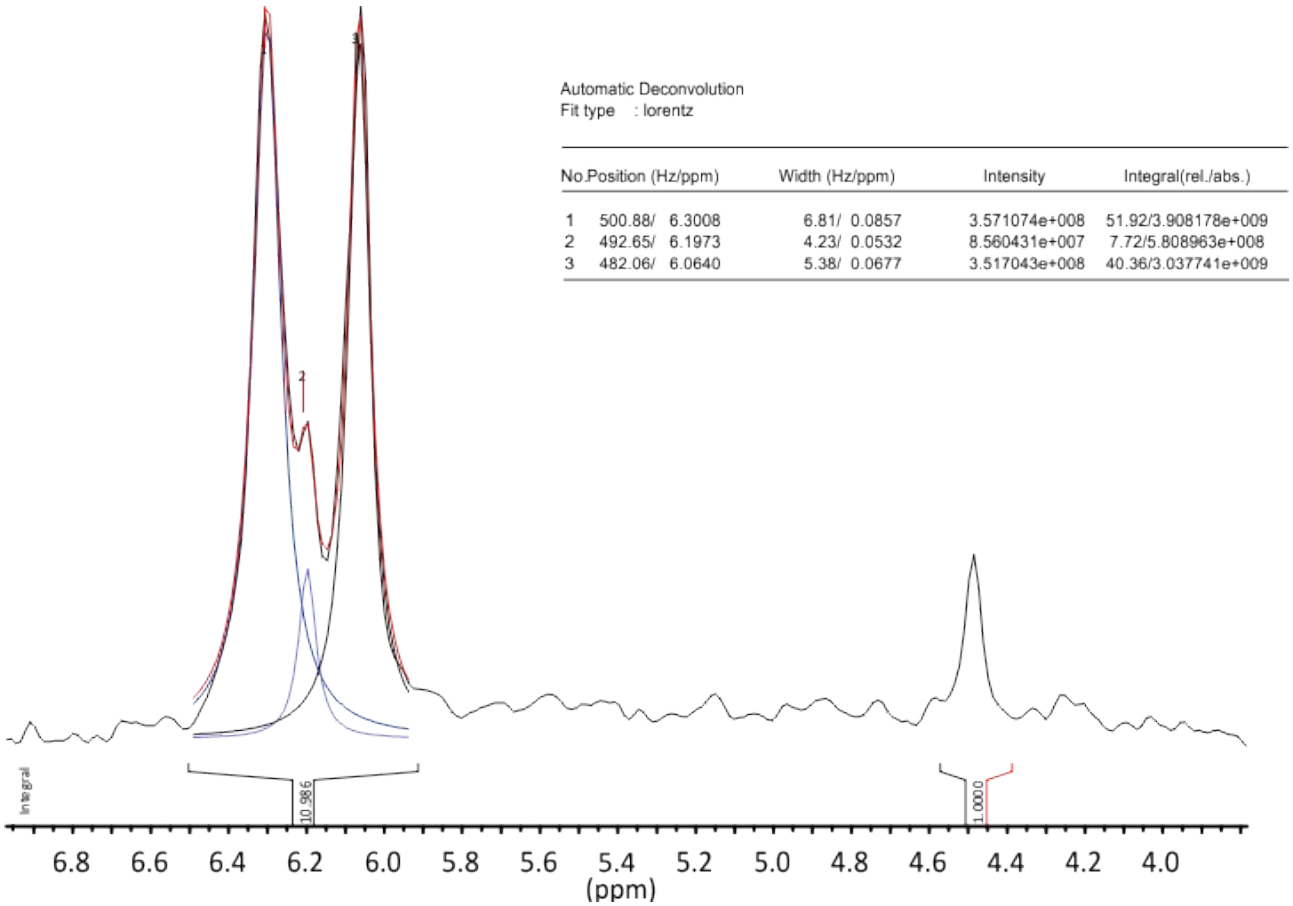

Figure S6. Result of deconvolution of $^{29}Si\{^{1}H\}$ NMR spectrum (79.5 MHz, toluene-d_8, –30 °C) of complex $\{ONO^{SiMe2tBu}\}Ti(CH_2Ph)(\eta^6\text{-Ph})CH_2B(C_6F_5)_3$ (**2-Ti**).

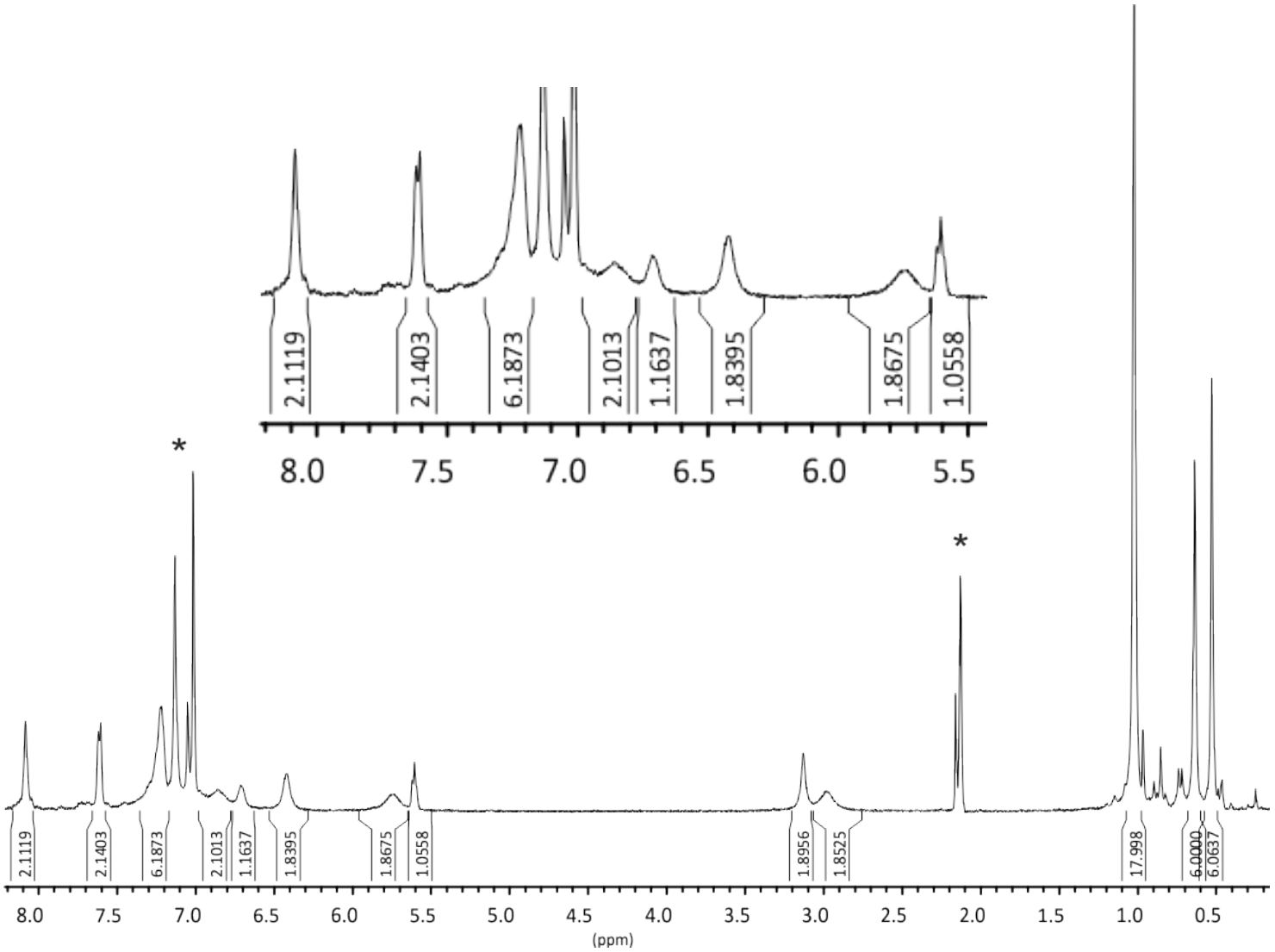

Figure S7. ^{1}H NMR spectrum (500 MHz, toluene-d_8, 25 °C) of complex {ONO$^{\mathrm{SiMe2}t\mathrm{Bu}}$}Zr($CH_2Ph$)($\eta^6$-Ph)$CH_2B(C_6F_5)_3$ (**2-Zr**) (* stand for solvent peaks).

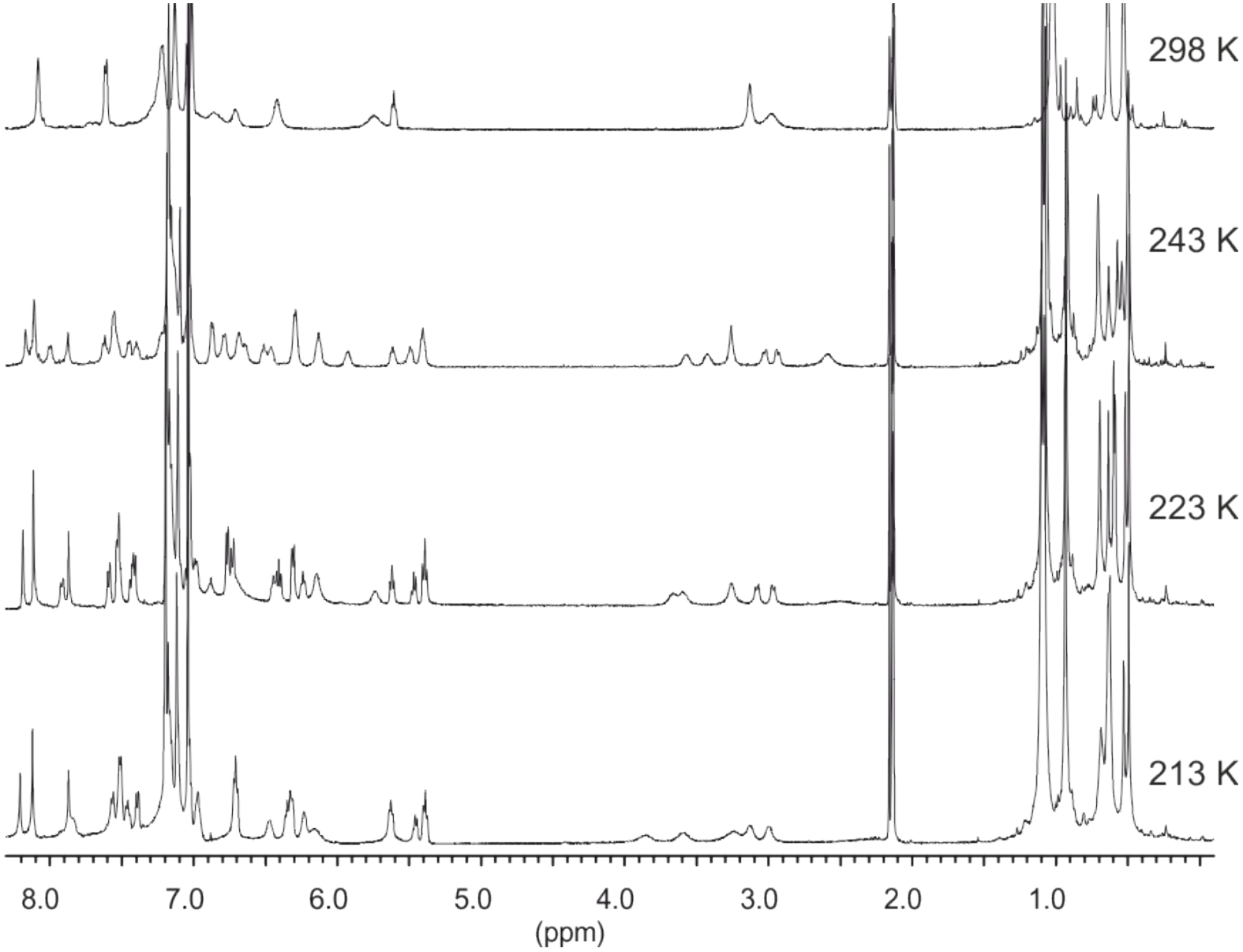

Figure S8. Stack plot of ^{1}H NMR spectra (500 MHz, toluene-d_8) of complex {ONO$^{\mathrm{SiMe2}t\mathrm{Bu}}$}Zr($CH_2Ph$)($\eta^6$-Ph)$CH_2B(C_6F_5)_3$ (**2-Zr**).

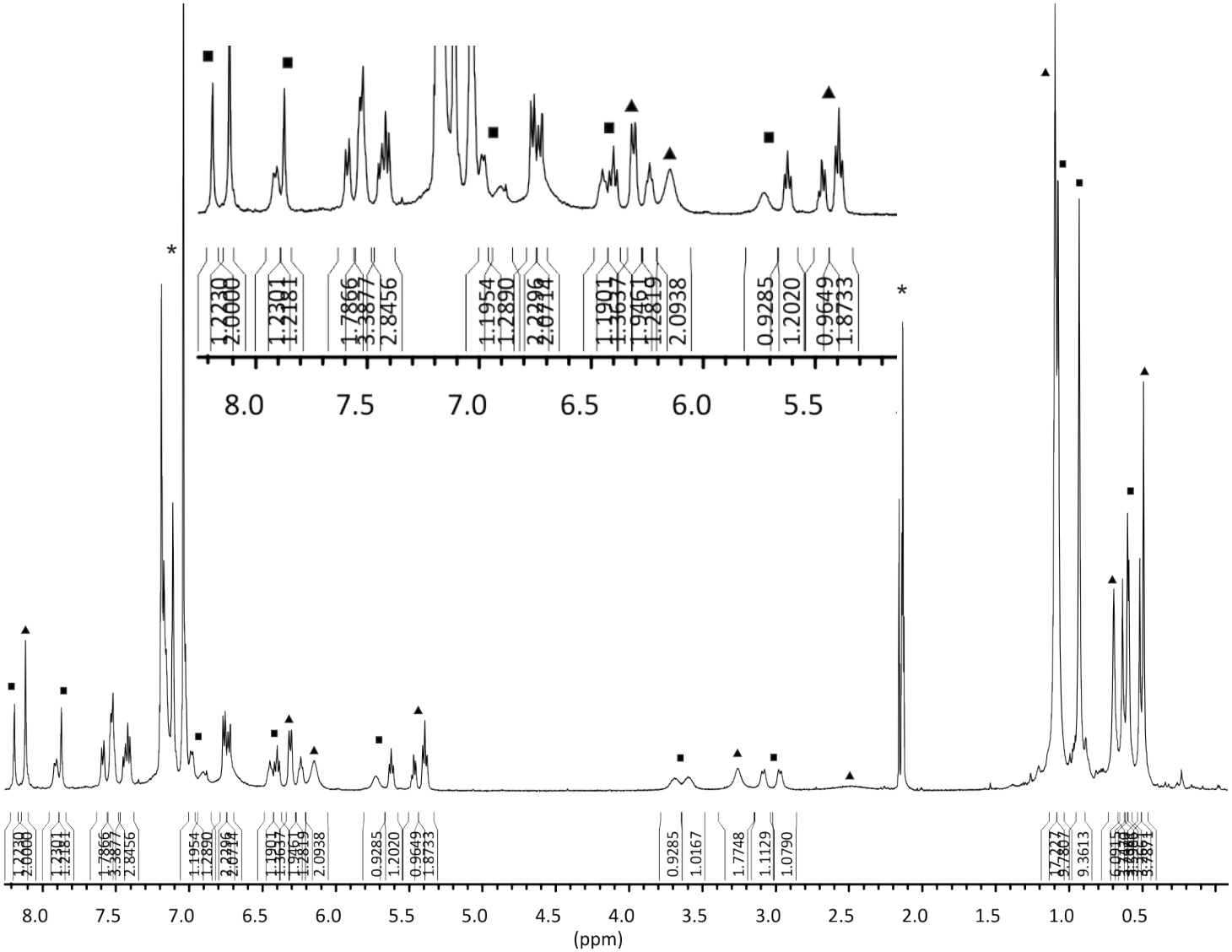

Figure S9. ^{1}H NMR spectrum (500 MHz, toluene-d_8, –50 °C) of complex {ONO$^{\mathrm{SiMe2}t\mathrm{Bu}}$}Zr($CH_2Ph$)($\eta^6$-Ph)$CH_2B(C_6F_5)_3$ (**2-Zr**) (* stand for solvent peaks).

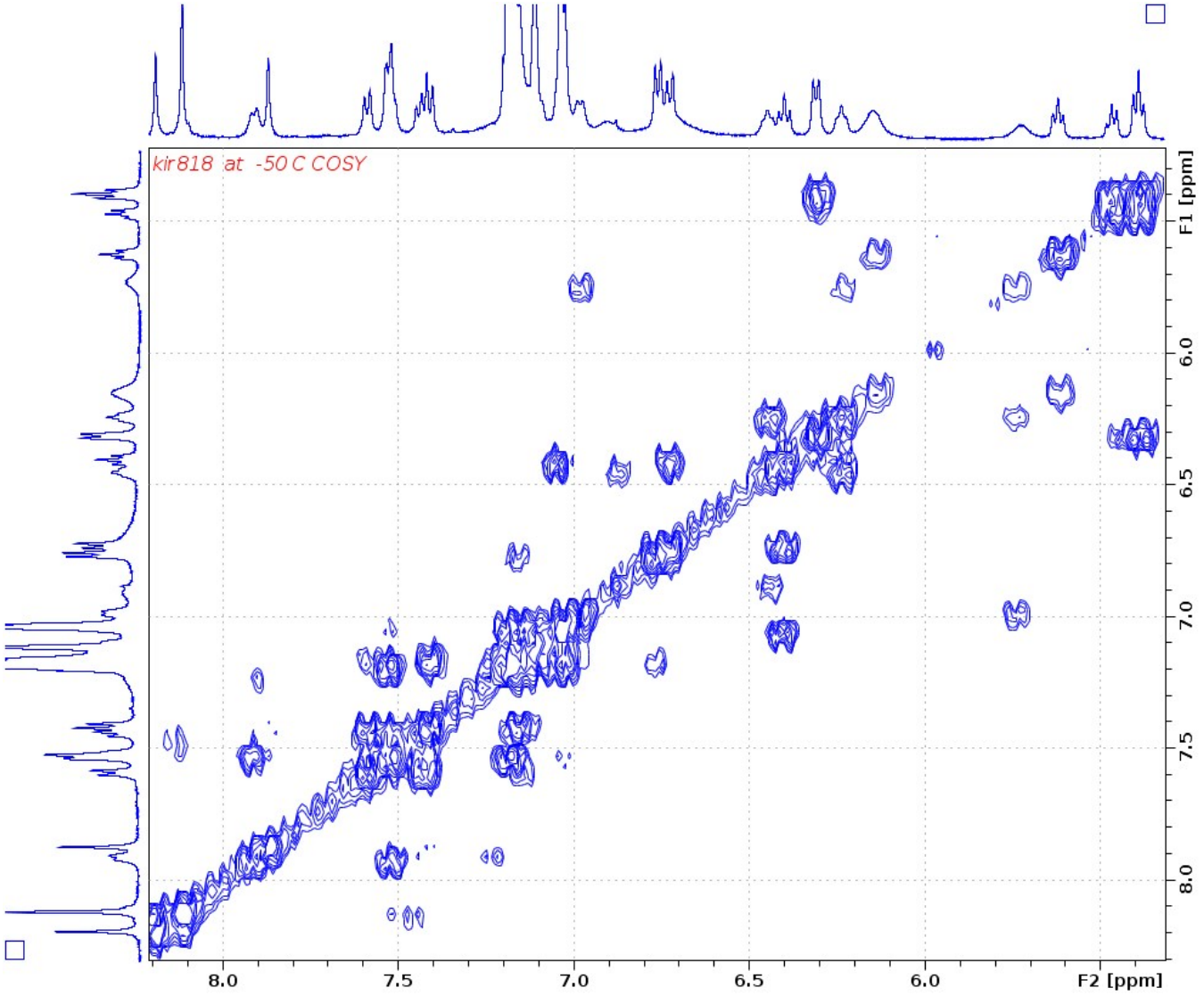

Figure S10. Low-field portion of the ^{1}H–^{1}H COSY NMR spectrum (500 MHz, toluene-d_8, –50 °C) of complex {ONO^{SiMe2tBu}}Zr(CH_2Ph)(η^6-Ph)$CH_2B(C_6F_5)_3$ (**2-Zr**).

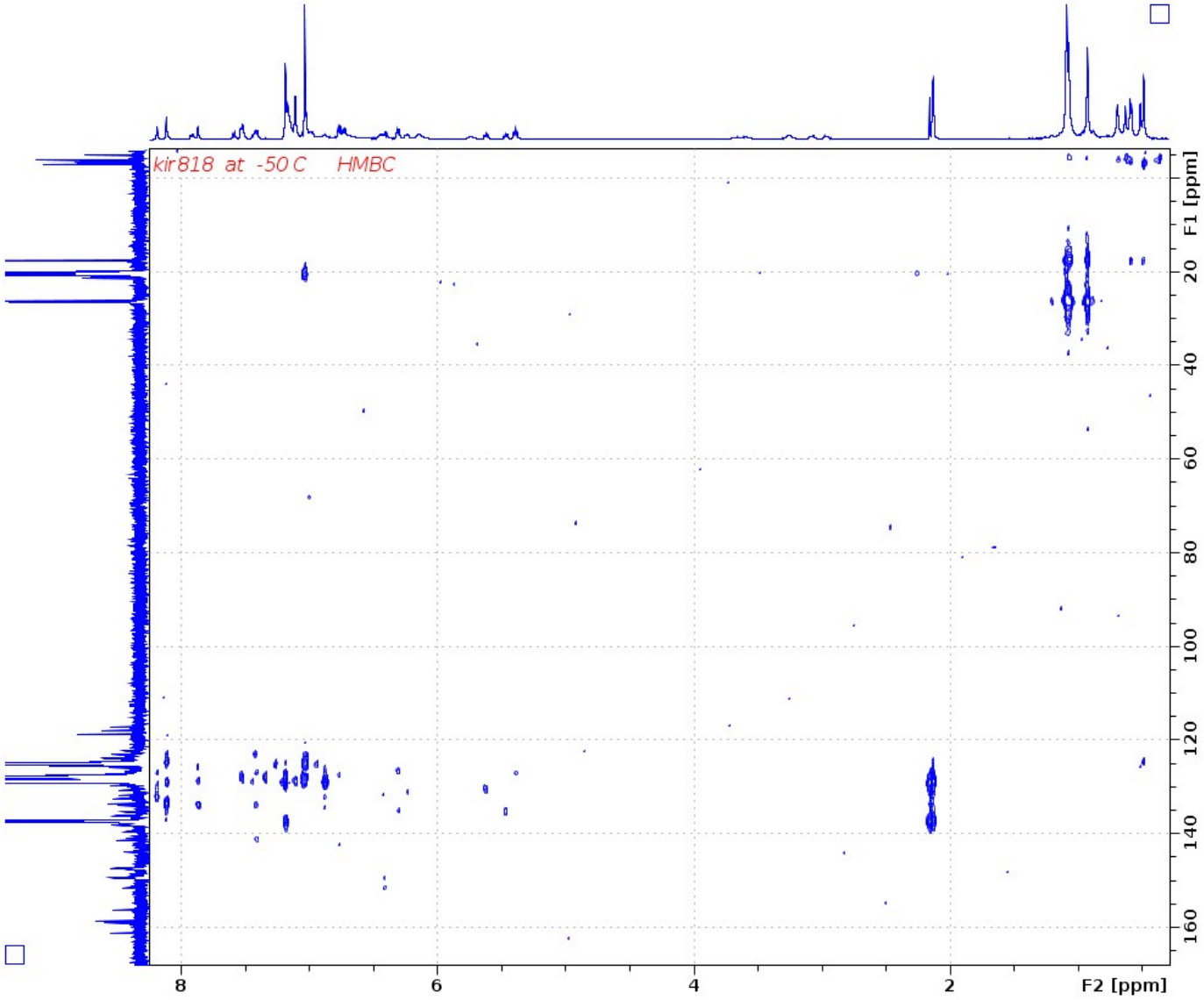

Figure S11. ^{1}H–^{13}C HMQC NMR spectrum (500 MHz, toluene-d_8, –50 °C) of complex {ONO^{SiMe2tBu}}Zr(CH_2Ph)(η^6-Ph)$CH_2B(C_6F_5)_3$ (**2-Zr**).

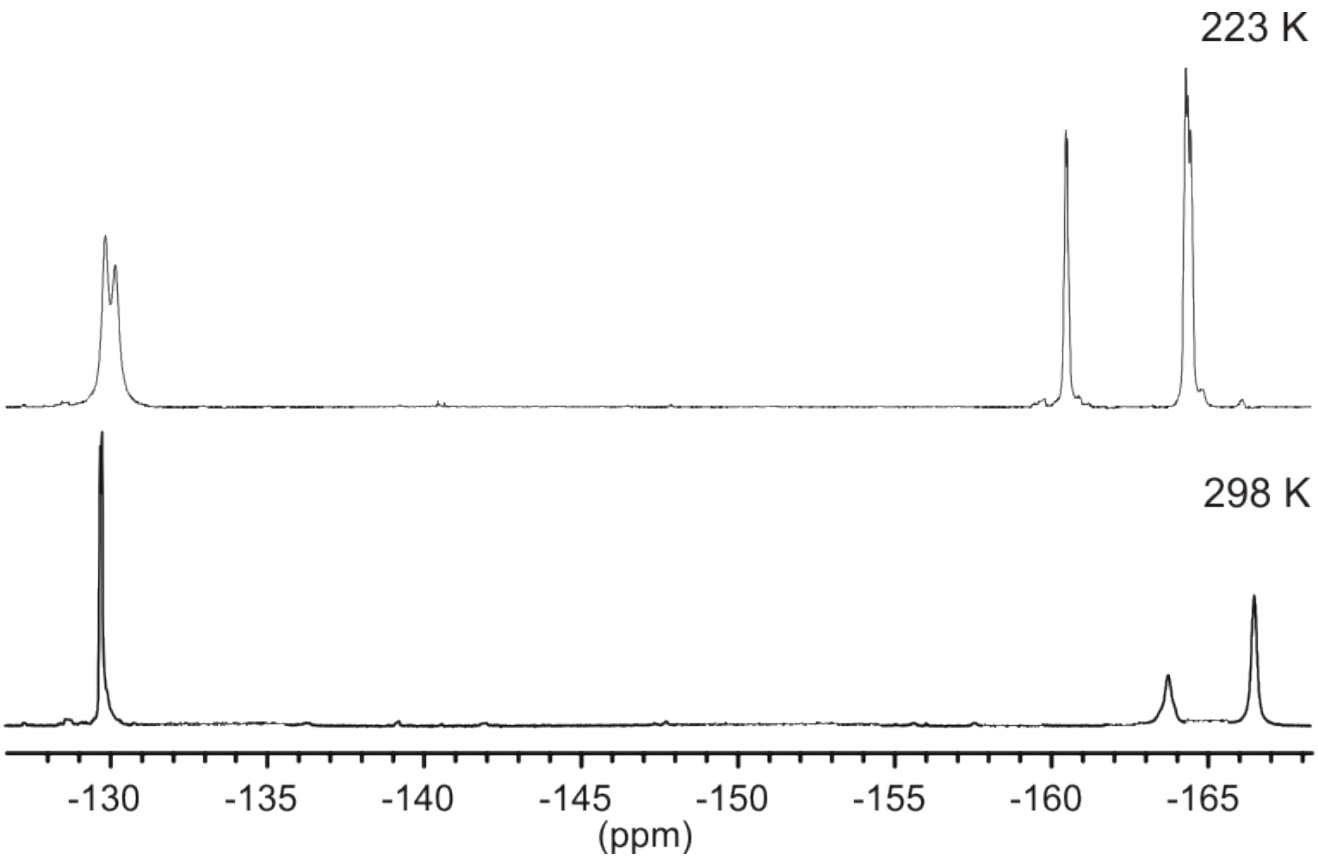

Figure S12. Stack plot of $^{19}F\{^{1}H\}$ NMR spectra (376 MHz, toluene-d_8) of complex $\{ONO^{SiMe2tBu}\}Zr(CH_2Ph)(\eta^6\text{-}Ph)CH_2B(C_6F_5)_3$ (**2-Zr**).

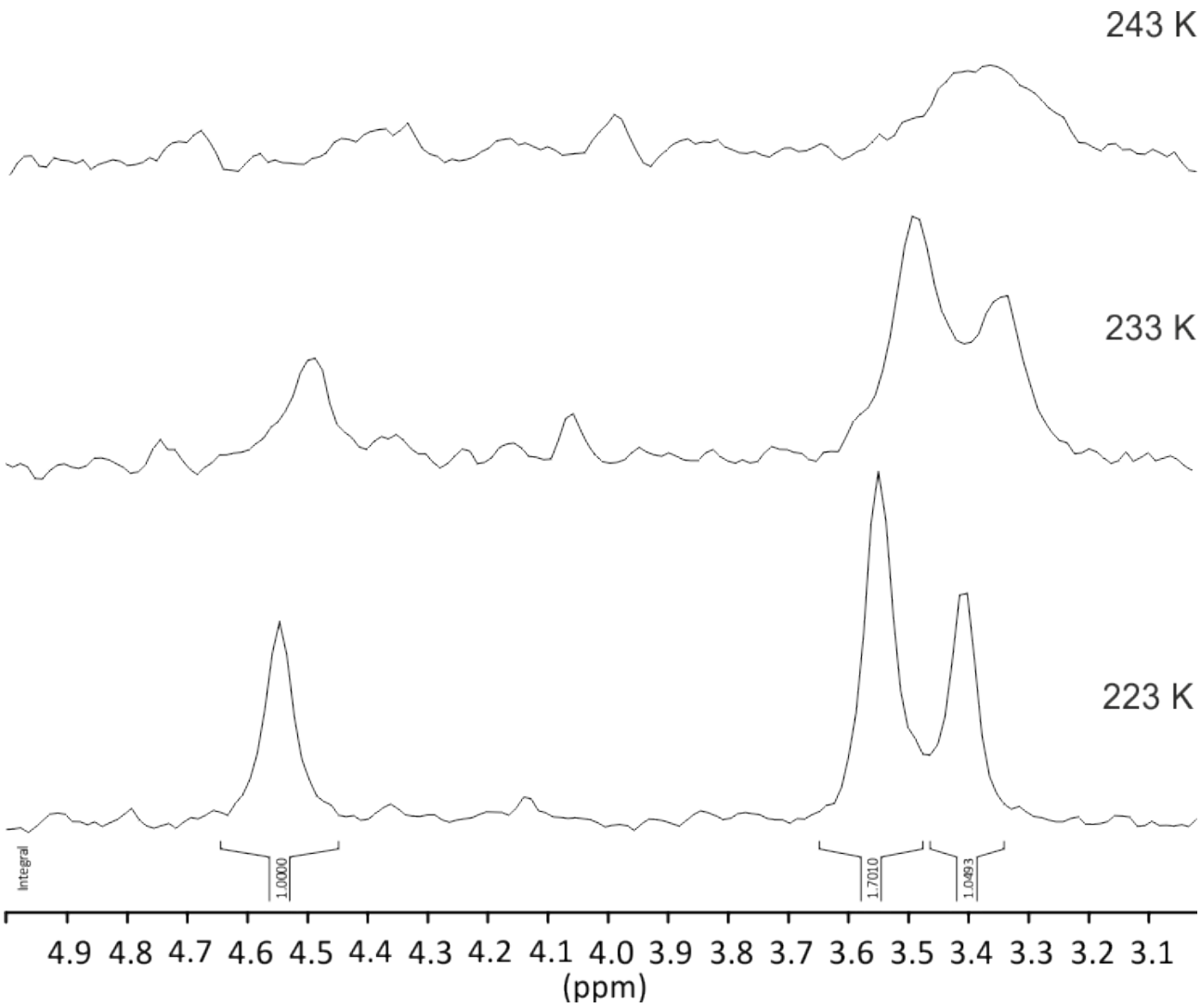

Figure S13. Stack plot of $^{29}Si\{^{1}H\}$ NMR spectra (79.5 MHz, toluene-d_8) of complex $\{ONO^{SiMe2tBu}\}Zr(CH_2Ph)(\eta^6\text{-}Ph)CH_2B(C_6F_5)_3$ (**2-Zr**).

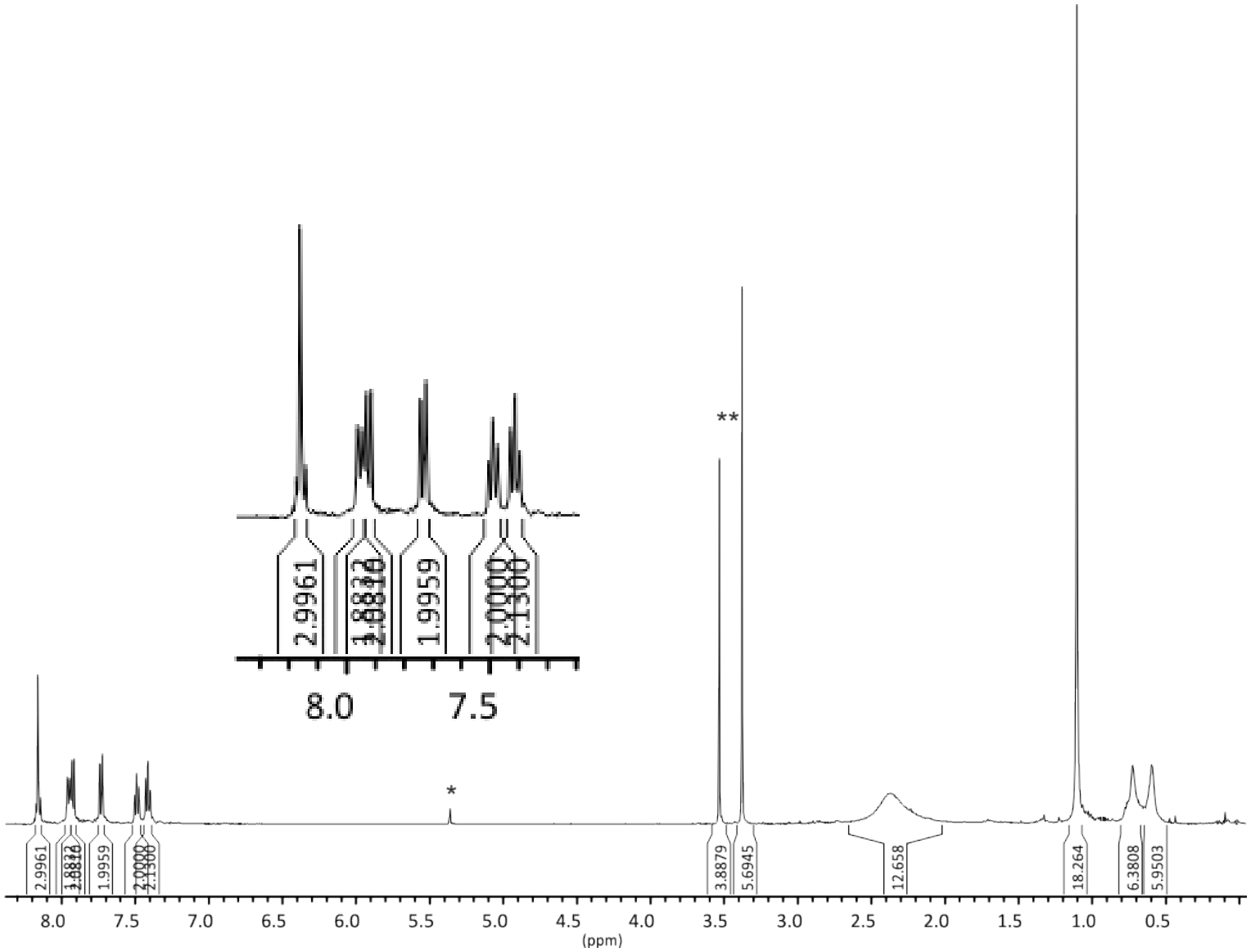

Figure S14. ^{1}H NMR spectrum (500 MHz, CD_2Cl_2, 25 °C) of complex {ONO^{SiMe2tBu}}$ZrCl_2(HNMe_2)$ **(3)** (* and ** stand for solvent and DME peaks, respectively).

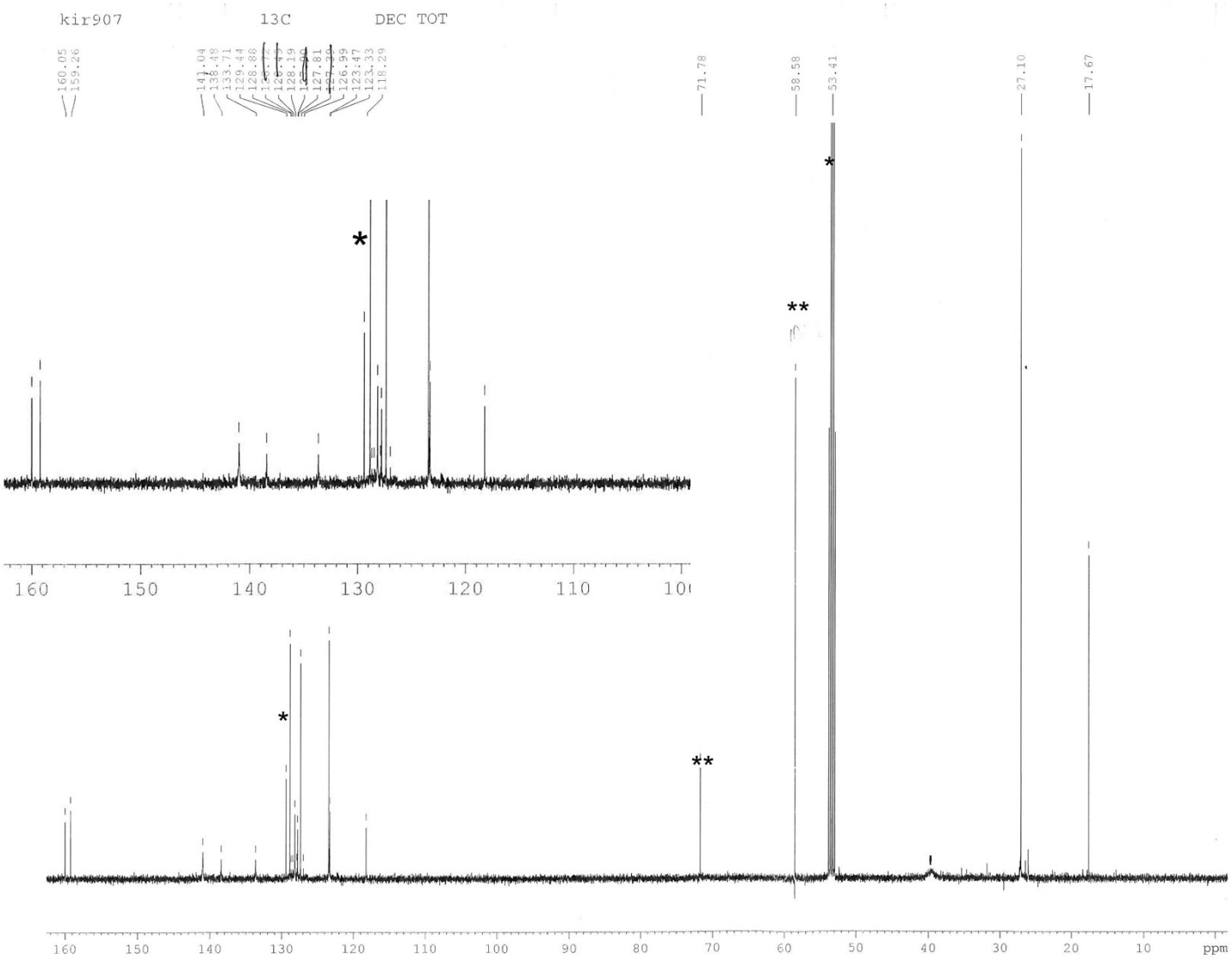

Figure S15. $^{13}C\{^{1}H\}$ NMR spectrum (125 MHz, CD_2Cl_2, 25 °C) of complex $\{ONO^{SiMe2tBu}\}ZrCl_2(HNMe_2)$ (**3**) (* and ** stand for solvent and residual DME peaks, respectively).

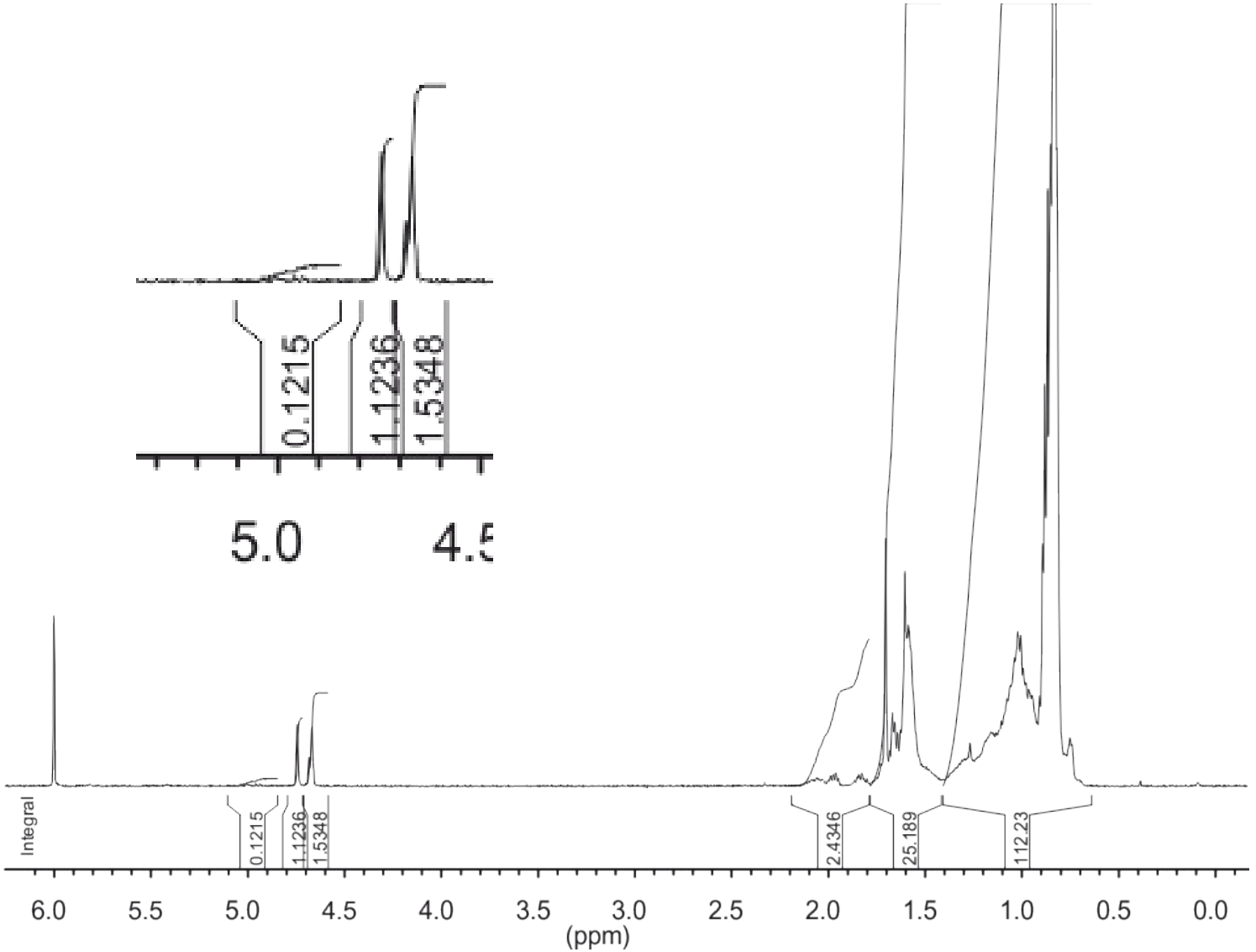

Figure S16. ^{1}H NMR spectrum (500 MHz, $C_2D_2Cl_4$, 25 °C) of oligopropylene sample prepared with **3**/MAO system (Table S2, entry 2).

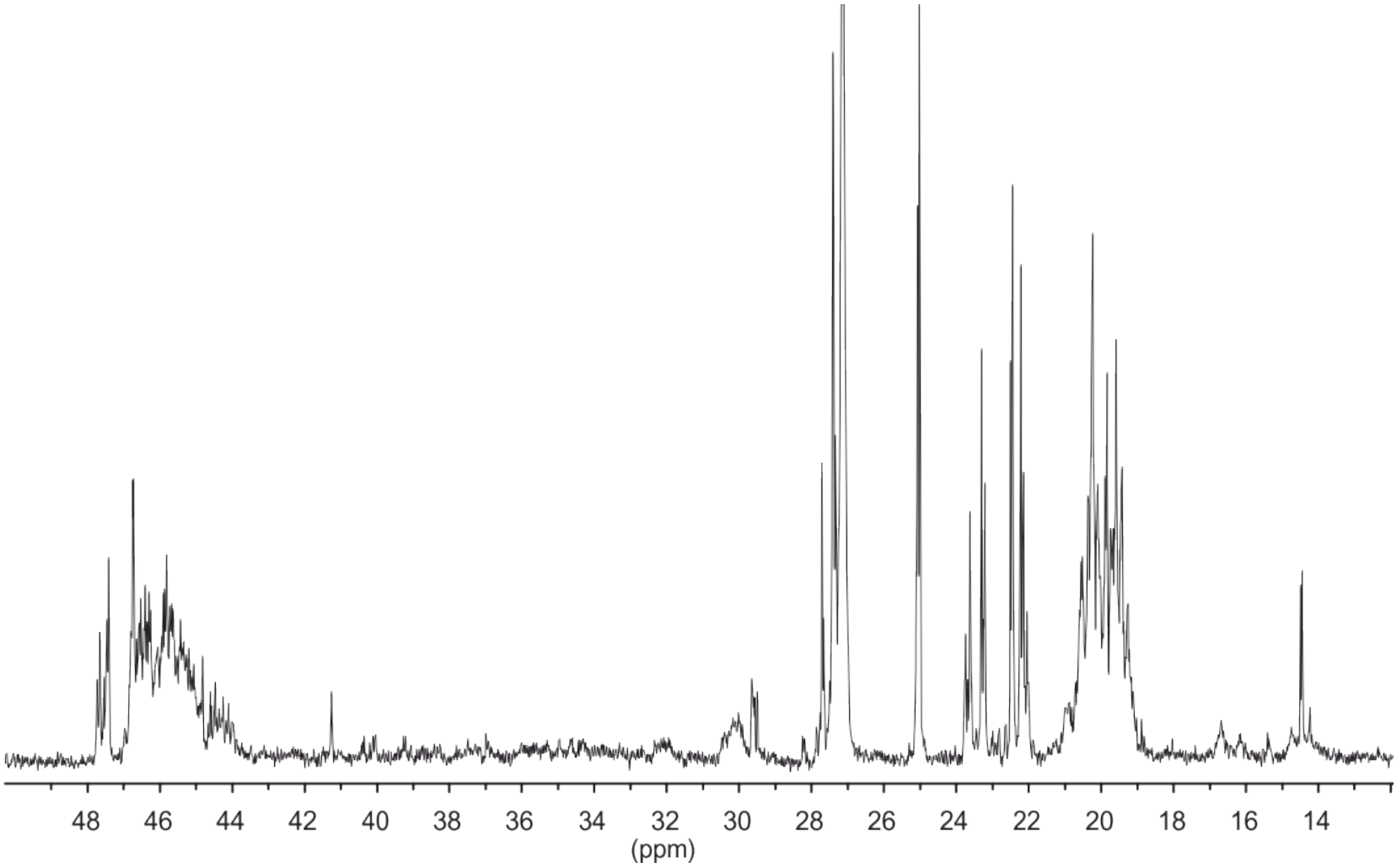

Figure S17. Aliphatic portion of the $^{13}C\{^{1}H\}$ NMR spectrum (125 MHz, $C_2D_2Cl_4$, 25 °C) of oligopropylene sample prepared with **3**/MAO system (Table S2, entry 2).

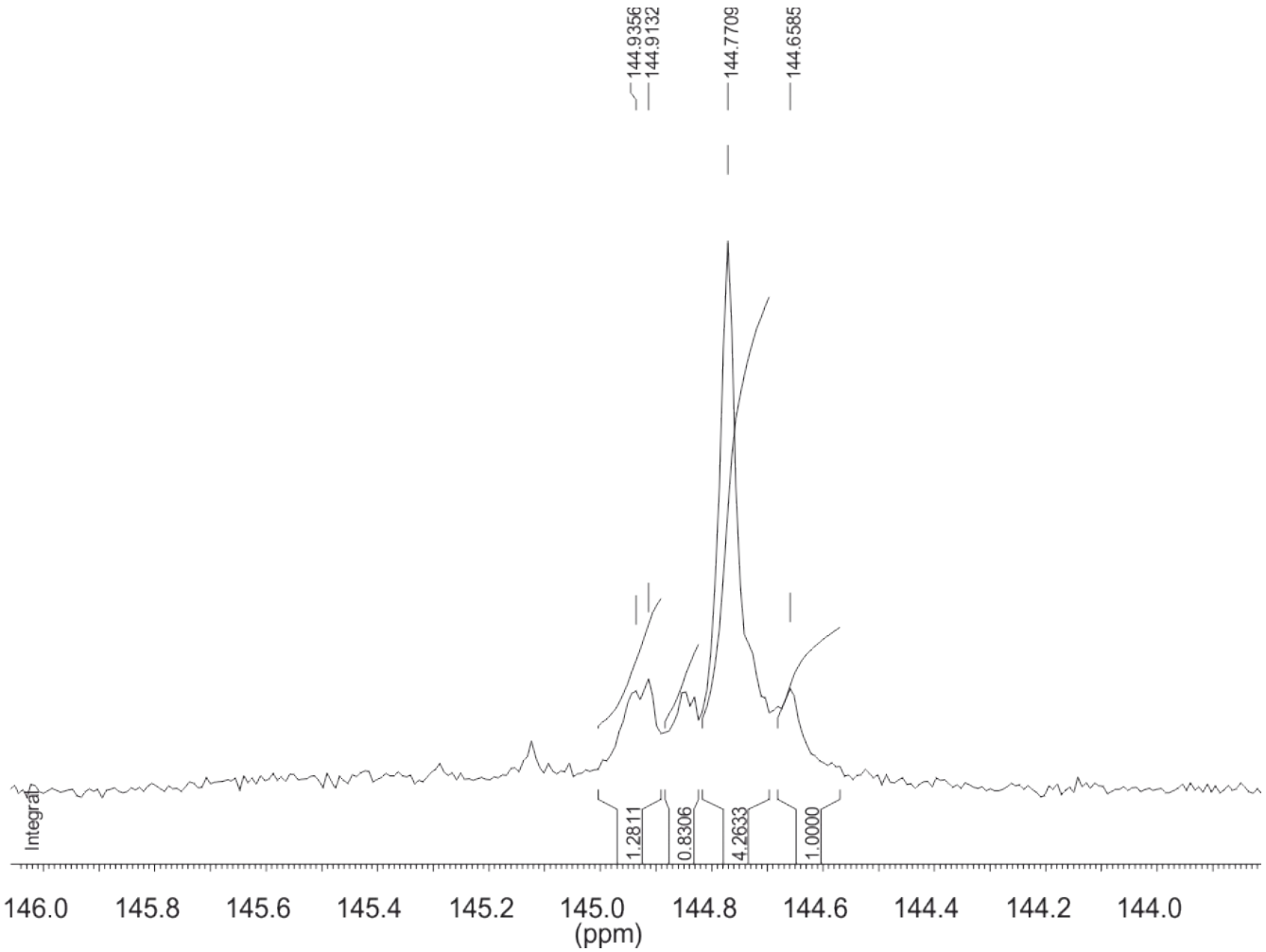

Figure S18. The *ipso*-carbon region of the $^{13}C\{^{1}H\}$ NMR spectrum (125 MHz, $C_2D_2Cl_4$, 25 °C) of polystyrene sample prepared with **3**/MAO system (Table S3, entry 19).

Table S1. Summary of Crystal and Refinement Data for Compounds **2-Zr** and **3**.

	2-Zr	**3**
Empirical formula	$C_{69}H_{57}BF_{15}NO_2Si_2Zr$	$3(C_{39}H_{50}Cl_2N_2O_2Si_2Zr)$, $7(C_6H_6)$
Formula weight	1375.37	2938.09
Temperature, K	150	150
Wavelength, Å	0.71073	0.71073
Crystal system	monoclinic	triclinic
Space group	P 2_1/c	P -1
a, Å	16.3881(4)	18.8689(10)
b, Å	28.2501(7)	20.4867(11)
c, Å	18.8581(5)	22.9343(13)
α, deg	90	69.667(2)
β, deg	115.6710(10)	75.579(2)
γ, deg	90	70.528(2)
Volume, Å^3	7868.9(3)	7748.1(7)
Z	4	2
Density (calc.), Mg/m^3	1.161	1.259
Absorption coefficient,mm^{-1}	0.243	0.403
Crystal size, mm^3	0.35 x 0.22 x 0.15	0.41 x 0.28 x 0.06
Reflections collected	121430	116649
Independent reflections	17983	34197
Max. and min. transmission	0.964 , 0.847	0.976 , 0.851
Data / restraints / parameters	17983 / 0 / 830	34197 / 21 / 1459
Final R indices [I>2σ(I)]	0.0472	0.0643
R indices (all data)	0.0716	0.1031
Goodness-of-fit on F^2	1.065	1.114
Largest diff. peak, e.Å^{-3}	0.519 and –0.416	2.259 and –2.184

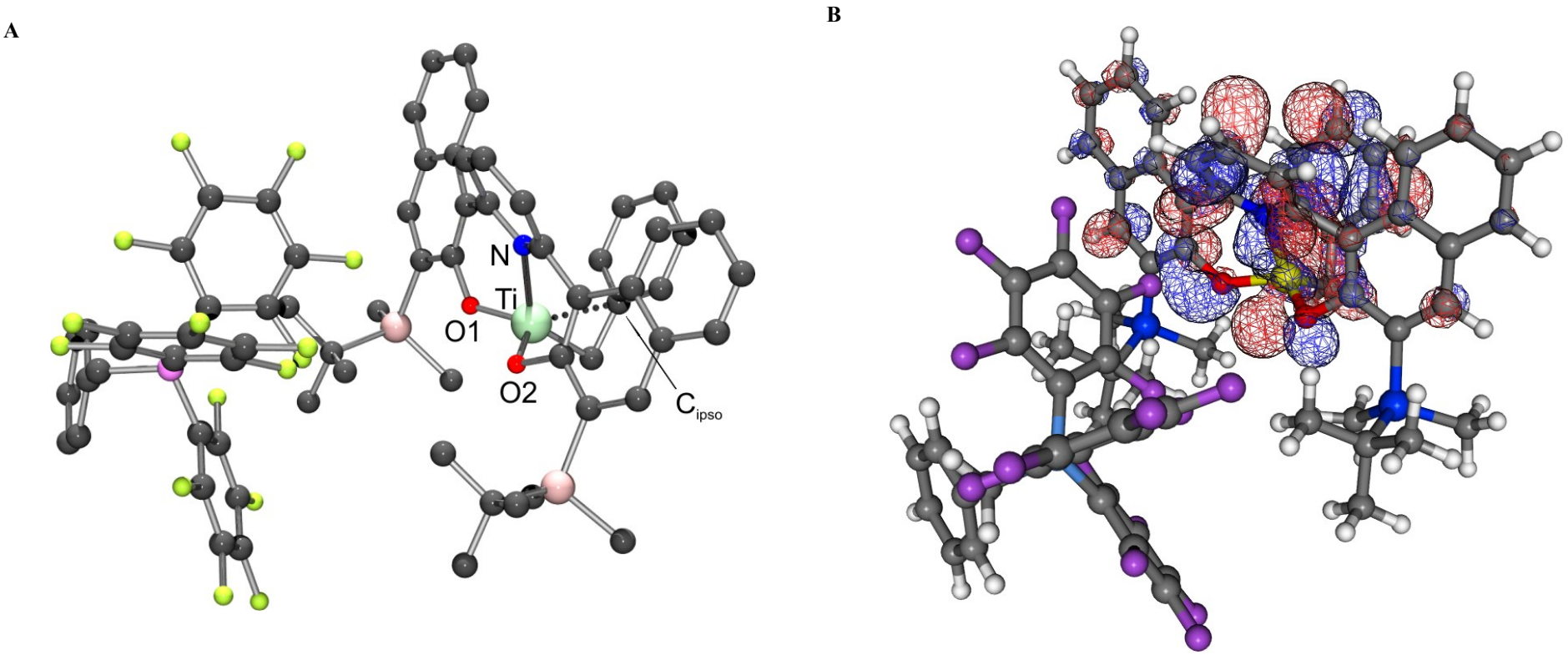

Figure S19. DFT data obtained from B3PW91 level calculations for OSIP **2-Ti-*C*$_s$-decoord(1)**: (A) Optimized structure (all hydrogen atoms are omitted for clarity). Selected bond distances (Å) and angles (°): C (benzyl)–Ti, 2.067; C_{ipso}(benzyl)–Ti, 2.440; N–Ti, 2.057; N–Ti–C(benzyl), 134.80; N–Ti–C_{ipso}(benzyl), 97.90; N–Ti–O, 88.71 and 92.33; (B) Kohn-Sham LUMO (isosurface value, 0.01; –0.1249 a.u.).

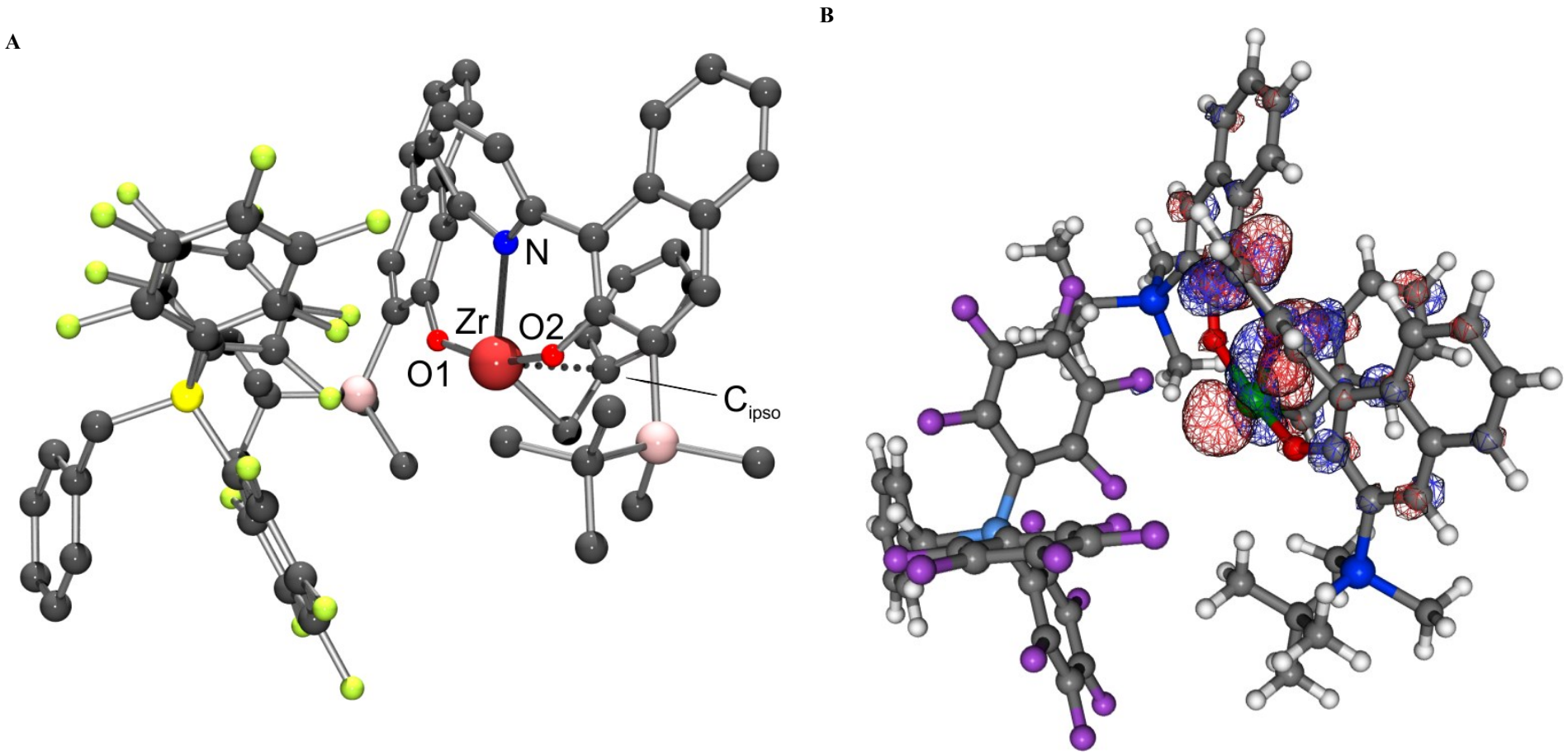

Figure S20. DFT data obtained from B3PW91 level calculations for OSIP **2-Zr-*C*$_s$-decoord(1)**: (A) Optimized structure (all hydrogen atoms are omitted for clarity). Selected bond distances (Å) and angles (°):C (benzyl)–Zr, 2.217; C_{ipso}(benzyl)–Zr, 2.657; N–Zr, 2.331; C–F…Zr, 3.066; N–Zr–C(benzyl), 124.43; N–Zr–C_{ipso}(benzyl), 105.84; N–Ti–O, 81.33 and 65.43; (B) Kohn-Sham LUMO (isosurface value, 0.02; –0.1072 a.u.).

Additional results on the polymerization activity studies. The catalytic performance of the isolated discrete ionic complexes **2-Ti** and **2-Zr** or those generated *in situ* from the charge neutral **1-Ti** and **1-Zr** and the corresponding molecular cocatalysts ($B(C_6F_5)_3$, $[Ph_3C]^+[B(C_6F_5)_4]^-$), was briefly evaluated in the homogeneous polymerization of alkenes (propylene and styrene).

In propylene polymerization (Table S2), the ternary system **1-Zr**/$[Ph_3C]^+[B(C_6F_5)_4]^-$/*i*Bu_3Al (used as scavenger) was found only barely active (entry 1). Whatever the activation mode in polymerization of styrene, that is either generation of active species *in situ* from **1-Ti** and $B(C_6F_5)_3$ or direct use of isolated **2-Ti**, no significant differences in terms of polystyrene yields or molecular weight properties were observed between the corresponding runs conducted in the temperature range of 25–80 °C (Table S3, compare entries 1, 3, 5 and 2, 4, 6, respectively). Most of the polymers obtained were soluble in THF, even at room temperature. In a few cases, polystyrene samples were found insoluble in acetone (entries 3–5), that is indicative of their stereoregular[1] (at least, in a part) structures. However, no melting transitions were detected in any case, which suggests that stereoregular sequences are short and/or randomly distributed within polymeric chain. The **1-Zr**/$B(C_6F_5)_3$ system was also found sluggishly active, though providing higher molecular weight atactic polymers (entries 7 and 8). In contrast with the titanium-based systems, no activity was observed for the zirconium-based analogue at 80 °C, which may reflect a lower thermal stability of this catalyst.

Polymerization of styrene using *in situ* combinations of the neutral **1-Ti** and **1-Zr** with $[Ph_3C]^+[B(C_6F_5)_4]^-$ was also studied. The system **1-Ti**/$[Ph_3C]^+[B(C_6F_5)_4]^-$ afforded small amounts of polystyrenes with molecular weight characteristics (M_n and M_w/M_n) close to those of the polymers obtained using cocatalyst $B(C_6F_5)_3$ (entries 10–12); on the other hand, **1-Zr**/$[Ph_3C]^+[B(C_6F_5)_4]^-$ appeared to be inactive at room temperature (entry 14). This discrepancy between the Ti- and Zr-based systems in polymerization of styrene can be a result of a generally higher intrinsic stability of Ti^{3+} species, the "true" precursors responsible for syndiospecific polymerization of styrene,[1,2] while the Zr-based systems are typically much less active.[1,3]

Table S2. Propylene Polymerization Promoted by **1-Zr** and **3**.[a]

Entry	Catalyst	Co-catalyst	Temp. [°C]	Time [h]	m_p [g]	Productivity [kg·mol^{-1}·h^{-1}]	M_n[b] [10^3 g·mol^{-1}]	M_w/M_n[b]
1	**1-Zr**	$[Ph_3C]^+[B(C_6F_5)_4]^-$/ iBu$_3$Al (1:100)	50	2	traces	-	-	-
2	**3**	MAO (1000)	50	1	1.35	135	1.4	1.23

[a] General conditions: 300 mL high pressure reactor; catalysts, 10 µmol; solvent toluene, 80 mL; P = 5 bars. [b] Determined by GPC.

Table S3. Styrene Polymerization Promoted by **1-Ti**, **1-Zr**, **2-Ti**, **2-Zr** and **3**.[a]

Entry	Catalyst	Co-catalyst	Temp. [°C]	Time [h]	Yield [g]	M_n [b] [10^3 g·mol^{-1}]	M_w/M_n [b]	T_m [c] [°C]	PS
1	**1-Ti**	$B(C_6F_5)_3$	25	18	0.08	24.4	3.9	-	aPS
2	**2-Ti**	-	25	18	0.10	43.7	2.8	n.o.	aPS
3	**1-Ti**	$B(C_6F_5)_3$	50	3	0.02	19.5	2.2	n.o.	sPS enriched
4	**2-Ti**	-	50	18	0.05	28.7	2.2	n.o.	sPS enriched
5	**1-Ti**	$B(C_6F_5)_3$	80	3	0.08	25.2	2.3	n.o.	sPS enriched
6	**2-Ti**	-	80	3	0.10	36.4	2.7	-	aPS
7	**1-Zr**	$B(C_6F_5)_3$	25	43	0.20	102	2.7	n.o.	aPS
8	**1-Zr**	$B(C_6F_5)_3$	50	24	0.10	205	2.6	n.o.	aPS
9	**1-Zr**	$B(C_6F_5)_3$	80	24	0	-	-	-	-
10	**1-Ti**	$[Ph_3C]^+[B(C_6F_5)_4]^-$	25	18	0.02	70.2	2.3	-	aPS
11	**1-Ti**	$[Ph_3C]^+[B(C_6F_5)_4]^-$	50	18	0.04	98.2	2.6	n.o.	aPS
12 [d]	**1-Ti**	$[Ph_3C]^+[B(C_6F_5)_4]^-$	50	18	0.08	49.5	2.7	-	aPS
13	**1-Ti**	$[Ph_3C]^+[B(C_6F_5)_4]^-$	80	18	0	-	-	-	-
14	**1-Zr**	$[Ph_3C]^+[B(C_6F_5)_4]^-$	25	18	0	-	-	-	-
15 [e]	**3**	MAO	50	15	1.23	9.9	1.2	n.o.	sPS enriched

[a] General conditions, otherwise stated: catalysts, 20 μmol; [B]/[Cat] = 1; [styrene]/[Cat] = 6500 (15 mL); Solvent = toluene (5 mL); n.o. = not observed. [b] Determined by GPC. [c] Determined by DSC. [d] catalyst, 40 μmol. [e] [styrene]/[Zr] = 3000; [Al]/[Zr] = 500.

References

1 Rodrigues, A.-S.; Kirillov, E.; Carpentier, J.-F. *Coord. Chem. Rev.* **2008**, *252*, 2115–2136.
2 Mahanthappa, M. K.; Waymouth, R. M. *J. Am. Chem. Soc.* **2001**, *123*, 12093–12094.
3 Schellenberg, J. *Prog. Polym. Sci.* **2009**, *34*, 688–718.